A Certified Model Reduction Approach
for robust optimal control with PDE constraints

Alessandro Alla

Department of Scientific Computing, Florida State University, Tallahassee FL-32306

Michael Hinze

Department of Mathematics, Universität Hamburg, Bundesstr. 55, 20146 Hamburg, Germany.

Oliver Lass

Department of Mathematics, Technische Universität Darmstadt, Dolivostr. 15, 64293 Darmstadt, Germany

Stefan Ulbrich

Department of Mathematics, Technische Universität Darmstadt, Dolivostr. 15, 64293 Darmstadt, Germany

Abstract

We investigate an optimal control problem governed by a parametric elliptic partial differential equation with uncertain parameters. We introduce a robust optimization framework that accounts for uncertain model and optimization parameters. The resulting optimization problem, then, has a bi-level structure for the solution of this problem which leads a non-linear optimization problem with a min-max formulation. The idea is to utilize a suitable approximation of the robust counterpart. However, this approach turns out to be very expensive, therefore we propose a goal-oriented model order reduction approach which avoids long offline stages and provides a certified reduced order surrogate model for the parametrized PDE which then is utilized in the numerical optimization. Numerical results are presented to validate the presented approach.

Keywords: model order reduction, optimal control, robust optimization, proper orthogonal decomposition
2000 MSC: 35Q93, 49J20, 49K20

Email addresses: `aalla@fsu.edu` (Alessandro Alla), `michael.hinze@uni-hamburg.de` (Michael Hinze), `lass@mathematik.tu-darmstadt.de` (Oliver Lass), `ulbrich@mathematik.tu-darmstadt.de` (Stefan Ulbrich)

1. Introduction

Optimal control governed by partial differential equations (PDEs) is a well-studied topic due to its relevance in industrial applications. If the model is considered to be *perfect* one can perform standard techniques to solve these type of problems (see e.g. [20, 39] and the references therein). However, its numerical approximation can be very expensive due to the dimension of the discretized PDE. For this reason, in the last decade, model order reduction techniques were introduced and successfully applied in the context of PDE constrained optimization. Model order reduction works in a Galerkin projection framework, where the basis functions are non-local and are build upon information of the underlying system. Although a detailed description of these contributions goes beyond the scope of this paper, we want to mention balance truncation which works mainly for linear state equations (see e.g. [4]). More general techniques are the reduced basis (RB) method and Proper Orthogonal Decomposition (POD). The latter is manly used in the context of e.g. many-query scenarios (see e.g. [36]) for parametric steady problems where the basis functions are selected by means of a greedy algorithm. The former works in more general situations such as time-dependent problems, and parametric steady and unsteady equations (see e.g. [42] for a presentation of the method within different applications). It is also possible to combine RB and POD in the so-called Greedy-POD algorithm [18] for parametric unsteady models. The strength of these methods is the presence of an a-posteriori error estimator which certifies the quality of the surrogate models. Model order reduction has been applied successfully to optimal control problems in both open-loop (e.g. [21, 25, 37]) and closed-loop (e.g. [3, 6, 27]) frameworks.

For the purpose of this work we assume that the PDE which governs our system is given but material imperfections are present. These are due to e.g. manufacturing and generate introduce uncertainty to the model. This problem arises in many real life applications. One way to include this uncertainty into the optimization process is through robust optimization. In this case no probabilistic model of the uncertainty is required. Instead, a deterministic approach is applied by assuming that the uncertainty is restricted to a bounded uncertainty set. Using the notion of a robust counterpart the associated original uncertain optimization problem is reformulated. The solution obtained in this way stays feasible for all realizations from the uncertainty set and at the same time yields the best worst-case value of the objective function. An alternative, to the presented approach are techniques which resolve the uncertainty by means of stochastic optimization e.g. [10, 26, 32, 40]. These methods depend on sampling the uncertain parameters and hence can become prohibitive expensive in the context of PDE constrained optimization. For a general discussion of robust optimization we refer to e.g. [7, 8, 9].

In this work the focus is on solving the robust counterpart in an efficient way which is a challenging task due to its bi-level structure. The idea is to utilize a suitable approximation of the robust counterpart, e.g. [12, 23, 28, 38, 44] or exploit specific properties e.g.[23]. We investagate the approximation of the

robust counterpart using a quadratic model. This allows us to reformulate the robust optimization problem as a *mathematical program with equilibrium constraints* (MPEC). This approach has been investigated in [28, 38] in the context of PDE constrained optimization problems. Our model will be a linear elliptic parametric equation where an affine decomposition will be applied to work with a reference parameter. The worst-case problem leads a non-linear optimization problem with a $\min - \max$ formulation. After approximating the inner maximization derivative based optimization is applied. In the setting of our work we will utilize a sensitivity based approach since we assume to deal with few parameters. This approach is computationally expensive because it requires the solution of a PDE for each parameter. Therefore model order reduction is applied in order to reduce the complexity of the optimization problem [43]. In this paper we consider the Proper Orthogonal Decomposition (POD) as a tool for model reduction (we refer to e.g. [42] for more details on the topic). In particular, we will build a goal-oriented algorithm which avoids expensive offline stages and updates the snapshot set in the direction of the suboptimal configuration. In this way the reduced order model is enhanced during the optimization to fit the requirements. The method is certified by an a-posteriori error estimator for the state variable and the sensitivities. Therefore, error estimators for the state and the sensitivities are required. A generalized error estimator is derived to cover these needs. Thanks to these estimators we are able to build the algorithm which provides efficient solutions reducing the complexity of the solution. This approach complements the method proposed in e.g. [28] where in each iteration of the optimization a new reduced order model is generated.

The paper is organized as follows: in Section 2 we present the mathematical model and in Section 3 we present the nominal and the robust optimization problem. Section 4 focuses on model order reduction for the optimization problem and in Section 5 we illustrate the effectiveness of the discussed methods by numerical examples.

2. Elliptic Parametric PDEs

In this section we introduce our abstract model problem: we deal with a linear elliptic equation with arbitrary boundary conditions, considering $\mathcal{D} \subset \mathbb{R}^M$, $M \geq 1$ as the parameter space and $\Omega(p)$ as a domain:

$$\begin{cases} \text{For } p \in \mathcal{D} \text{ find } \tilde{u} \in X(\Omega(p)) \text{ s.t} \\ \tilde{a}(\tilde{u}, v; p) = \tilde{f}(v; p), \quad \forall v \in X(\Omega(p)), \end{cases} \tag{1}$$

where X is a suitable Hilbert Space, X' its dual space, $p \in \mathbb{R}^{N_p}$ a N_p dimensional parameter, Ω a regular bounded parameter dependent domain, $\tilde{u}$ the unknown variable, $\tilde{a} : X \times X \times \mathcal{D} \to \mathbb{R}$ is a bilinear bounded and coercive form on X and $f \in X'$ are given by

$$a(w, v; p) = \int_{\Omega(p)} \nabla w \nabla v \, \mathrm{d}x \quad \text{and} \quad f(v; p) = \int_{\Omega(p)} f v \, \mathrm{d}x.$$

3

Note that under these assumptions problem (1) admits a unique solution.

The function space X is such that $H_0^1(\Omega(p)) \subset X \subset H^1(\Omega(p))$, with

$$H^1(\Omega(p)) := \left\{ f \in L^2(\Omega(p)) : D^\alpha f \in L^2(\Omega(p)), \alpha \leq 1 \right\},$$

where f is a measurable function, $D^\alpha f$ denotes the weak $\alpha^{th}-$ partial derivative of f and the functional spaces $L^2(\Omega(p))$, $H_0^1(\Omega(p))$ are defined as follows:

$$L^2(\Omega(p)) := \left\{ f : \Omega(p) \to \mathbb{R}, \int_{\Omega(p)} f(x)^2 \, \mathrm{d}x < \infty \right\},$$

$$H_0^1(\Omega(p)) := \left\{ f \in H^1(\Omega(p)) : f \equiv 0 \text{ a.e. on } \partial\Omega(p) \text{in the sense of traces} \right\}.$$

In order to obtain a computationally fast model and to avoid remeshing when the parameter changes we require an affine decomposition which transforms problem (1) to a fixed reference domain $\bar{\Omega}$ by means of a linear transformation. For this purpose, let us assume that there is a piecewise-affine transformation

$$\mathcal{T} : \bar{\Omega} \to \Omega(p),$$

such that $\Omega(p) = \mathcal{T}(p)\bar{\Omega}$. Without loss of generality, we will consider only one reference domain. As it is shown in e.g. [36], the parametric map $\mathcal{T}(p)$ and its Jacobian $J_{\mathcal{T}}$ allow the definition of the bilinear and linear forms on the reference domain $\bar{\Omega}$.

Then, due to the linear transformation our problem reads:

$$\begin{cases} \text{For } p \in \mathcal{D} \text{ find } u \in X(\bar{\Omega}) \text{ s.t.} \\ a(u, v; p) = f(v; p), \quad \forall v \in X(\bar{\Omega}), \end{cases} \tag{2}$$

where the assumptions in problem (1) hold true. Note that the relations between $a(\cdot, \cdot, p)$ and $\tilde{a}(\cdot, \cdot, p)$ and for the right hand side f and $\tilde{f}$ are given by

$$a(u, v; p) = \tilde{a}(J_{\mathcal{T}}^{-1}u, J_{\mathcal{T}}^{-1}v; p)|J_{\mathcal{T}}| \quad \text{and} \quad f(v; p) = \tilde{f}|J_{\mathcal{T}}|.$$

Hence the bilinear form $a(\cdot, \cdot; p)$ can be expressed with an affine linear decomposition:

$$a(u, v; p) = \sum_{q=1}^{Q} \Theta_a^q(p) a_q(u, v), \tag{3}$$

such that $\Theta^q : \mathcal{D} \to \mathbb{R}$ for $q = 1, \ldots, Q$ is a function depending on p and $a_q : X \times X \to \mathbb{R}$ is parameter independent continuous bilinear form, i,e.,

$$a_q(u, v) := \tilde{a}_q(u, v; p^*),$$

where p^* is the reference parameter associate to the reference geometry. To allow such decompositions, the computational domain is decomposed into Q non-overlapping subdomains. This hypothesis on $a(\cdot, \cdot; p)$ allows us to improve the computational efficiency in the evaluation of $a(u, v; p)$: the components

$a^q(u, v)$ can be computed once and then are stored in the so called offline stage of the method. In other words we assume that the problem is affine dependent on the parameter p. The same affine decomposition is applied to f with

$$f(v; p) = \sum_{q=1}^{Q} \Theta_f^q(p) f_q(v)$$

with $f^q(v) := \tilde{f}(v; p^*)$. This assumption is the key for the purpose of model reduction as we will see in Section 4. Furthermore, we define the coercivity constant that will be a key ingredient in the certification of the model reduction algorithm, by

$$\alpha(p) := \inf_{w \in X(\bar{\Omega})} \frac{a(w, w; p)}{\|w\|_{X(\bar{\Omega})}}, \tag{4}$$

and the continuity constant as

$$\gamma(p) := \sup_{v \in X(\bar{\Omega})} \sup_{w \in X(\bar{\Omega})} \frac{a(w, v; p)}{\|w\|_{X(\bar{\Omega})} \|v\|_{X(\bar{\Omega})}}. \tag{5}$$

For the purpose of the optimization problem we will compute the sensitivities $u_i^1 := \frac{\partial u(p)}{\partial p_i}$ which are obtained by the derivative with respect to the parameters from equation (2) leading the following linear problem:

$$\begin{cases} \text{For } p \in \mathcal{D} \text{ find } u_i^1 \in X(\bar{\Omega}) \text{ s.t.} \\ a(u_i^1, v; p) = \frac{\partial f}{\partial p_i}(v; p) - \frac{\partial a}{\partial p_i}(u, v; p), \quad \forall v_h \in X(\bar{\Omega}), \ i = 1, \ldots, N_p. \end{cases} \tag{6}$$

We note that due to the affine decomposition the i-th partial derivative of $a(\cdot, \cdot; p)$ and $f(\cdot; p)$ are given by the derivatives of coefficient functions Θ_a^q and Θ_f^q, $q = 1, \ldots, Q$ and can be computed analytically. More general, the n-th sensitivity can be computed by the following proposition. For this purpose, to ease notation, let us assume that $p \in \mathbb{R}$ and therefore drop the index i. For p vector valued the notation is cumbersome and does not add any scientific value.

Proposition 2.1. *Let the coefficient functions $\Theta_a^q(p)$ and $\Theta_f^q(p)$, $q = 1 \ldots, Q$, be n-times differentiable with respect to p. Then the solution u is differentiable with respect to p and the sensitivities $u^n = \frac{\partial^n u}{\partial p^n} \in X$ satisfy the sensitivity equation*

$$a(u^n, v; p) = \frac{\partial^n f}{\partial p^n}(v; p) - \sum_{k=1}^{n} \binom{n}{k} \frac{\partial^k a}{\partial p^k}(u^{n-k}, v; p), \tag{7}$$

where $\binom{n}{k} = \frac{n!}{k!(n-k)!}$ denotes the binomial coefficient.

The proof of the proposition follows from the general Leibniz rule for the n-th derivative applied to (3) and is omitted here. Let us note that $\binom{n}{k} := 0$ if $0 \leq n < k$. We can easily see that for $n = 0$ we find the state equation (2) and for $n = 1$ the first sensitivity equation (6).

5

Next, we introduce an high dimensional finite element (FE) discretization of our model problem in the space $X_h \subset X$. The discrete problem then reads

$$\begin{cases} \text{For } p \in \mathcal{D} \text{ find } u_h \in X_h(\bar{\Omega}) \text{ s.t.} \\ a(u_h, v_h; p) = f(v_h; p), \quad \forall v_h \in X_h(\bar{\Omega}). \end{cases} \tag{8}$$

For the discrete problem we use the ansatz $u_h = \sum_{i=1}^{N}(\mathbf{u}_h)_i \varphi_i$, where φ_i are suitable FE ansatz functions. Problem (8) then is equivalent to the linear system:

$$\begin{cases} \text{For } p \in \mathcal{D} \text{ find } \mathbf{u}_h \in \mathbb{R}^N \text{ s.t.} \\ \mathbf{K}(p)\mathbf{u_h}(p) = \mathbf{f}(p), \end{cases} \tag{9}$$

where $\mathbf{K}(p) \in \mathbb{R}^{N \times N}$ is the stiffness matrix $(\mathbf{K}(p))_{ij} = a(\varphi_i, \varphi_j; p)$, $1 \le i, j \le N$, and the right hand side $\mathbf{f}(p) \in \mathbb{R}^N$ is obtained by $(\mathbf{f}(p))_i = f(\varphi_i; p)$, $1 \le i \le N$. The FE system matrix keeps the dependency on the parameter p and we apply the affine decomposition to it in the following way

$$\mathbf{K}(p) = \sum_{q=1}^{Q} \Theta_a^q(p)\mathbf{K}_q, \tag{10}$$

where $\mathbf{K}_a^q$, $q = 1, \dots, Q$, are the system matrices on the Q sub-domains. We can note again that the p dependency of $\mathbf{K}$ is now only in the weight functions Θ_a^q which are easy and inexpensive to evaluate. We note that the same decomposition is made for the right hand side. Similarly, the discretized version of equation (6) reads:

$$\mathbf{K}(p)\mathbf{u}_{h,i}^1(p) = \tilde{\mathbf{f}}_i^1, \quad \text{for } i = 1, \dots, N_p, \tag{11}$$

which have to be solved with

$$\tilde{\mathbf{f}}_i^1 = \frac{\partial \mathbf{f}}{\partial p_i}(p) - \frac{\partial \mathbf{K}}{\partial p_i}(p)\mathbf{u}_h \quad \text{for } i = 1, \dots, N_p,$$

where N_p is the number of parameters in the problem and the subindex p_i indicates the derivative with respect to the i-th parameter. Note that these derivatives are easy to compute due to the previously introduced affine decomposition (10). The derivative of the matrix $\mathbf{K}(p)$ and the vector $\mathbf{f}(p)$ are given by the derivatives of the functions $\Theta_a^q(p)$ and $\Theta_f^q(p)$, $q = 1, \dots, Q$, respectively. For the general sensitivity equations (7) we get

$$\mathbf{K}(p)\mathbf{u}_h^n = \frac{\partial^n \mathbf{f}}{\partial p^n}(p) - \sum_{k=1}^{n} \binom{n}{k} \frac{\partial^k \mathbf{K}}{\partial p^k}(p)\mathbf{u}_h^{n-k}. \tag{12}$$

In the rest of the work we will work with the following following compact notation when appropriate:

$$\frac{\partial^n \mathbf{u}_h}{\partial p_i^n} := \mathbf{u}_{h,i}^n$$

in order to define the $n-th$ derivative of $\mathbf{u}_h$ with respect to the $i-th$ parameter. Similarly, we will adopt $\mathbf{f}_i^n$ and $\mathbf{K}_i^n$.

From now on we will focus on the discrete version (9) of the problem (1). All further steps are analogous in the continuous setting.

3. Optimization problem

In this section we formulate an optimization problem governed by a parametrized PDE. We will investigate the nominal optimization and its robust counterpart. The robust optimization problem takes uncertainties in model parameters into account by utilizing a worst-case formulation. In this context we investigate approximation techniques of different orders.

3.1. The nominal optimization

The nominal optimization problem under investigation is of the form

$$
\min_{p\in\mathbb{R}^{N_p},\mathbf{u}_h\in\mathbb{R}^{N_x}} \tilde{g}_0(p,\mathbf{u}_h), \quad \text{subject to (s.t.)} \quad \left\{ \begin{array}{ll} \tilde{g}_i(p,\mathbf{u}_h) \leq 0, & i=1,\ldots,N_g, \\ e(p,\mathbf{u}_h)=0, & \end{array} \right.
\tag{13}
$$

where $\tilde{g}_0$ is the objective function, $\tilde{g}_i$ are the $N_g \in \mathbb{R}$ inequality constraints, and e the equality constraint governed by the discretized parametric PDE in (9). Further, let $\tilde{g}_i$, $i=0,\ldots,N_g$ and e be continuously differentiable and let the Jacobian $\frac{\partial}{\partial u}e(p,u)$ be invertible. In this work we focus on the finite dimensional formulation since the main contributions are the incorporation of uncertainties and model order reduction.

Let $e(p,\mathbf{u}_h)=0$ have a unique solution $\mathbf{u}_h = \mathbf{u}_h(p)$ for every admissible p. Then we can introduce the reduced objective and constraint functions

$$
g_i(p) := \tilde{g}_i(p,\mathbf{u}_h) \quad \text{for} \quad i=0,\ldots,N_g.
$$

Consequently, the reduced optimization problem associated with (13) reads as

$$
\min_{p\in\mathbb{R}^{N_p}} g_0(p), \quad \text{s.t.} \quad g_i(p) \leq 0, \quad i=1,\ldots,N_g.
\tag{14}
$$

Since e is continuously differentiable with invertible Jacobian $\frac{\partial}{\partial u}e(p,u)$, the implicit function theorem guarantees that also $\mathbf{u}_h$ is continuously differentiable with respect to the parameter. Hence the reduced objective and the reduced constraints $g_i(p)$, $i=0,\ldots,N_g$, are continuously differentiable. The reduced formulation is the basis for the further investigation of the robust counterpart.

3.2. The robust optimization

Now we get to the robust optimization. For this purpose we associate a parameter ϕ with the model that is not exactly known and is subject to uncertainty. In our case the parameter ϕ describes a model parameter and hence enters the problem formulation through the equality constraint, i.e., $e(p,\mathbf{u}_h;\phi)=0$. The goal is to formulate the robust version of (14). To begin with, we assume some prior knowledge about the uncertain parameter. We assume that the uncertain parameter remains within a given uncertainty set

$$
\mathcal{U}_k = \left\{ \phi \in \mathbb{R}^{N_\phi} \,\big|\, \|D^{-1}(\phi - \hat{\phi})\|_k \leq 1 \right\} = \left\{ \phi \in \mathbb{R}^{N_\phi} \,\big|\, \phi = \hat{\phi} + \delta, \|D^{-1}\delta\|_k \leq 1 \right\},
\tag{15}
$$

where $\hat{\phi}$ is a nominal value and $k \in \{2,\infty\}$.

Remark 3.1. *Choosing $D = \mathrm{diag}((\overline{\phi} - \underline{\phi})/2)$, $\hat{\phi} = (\underline{\phi} + \overline{\phi})/2$ and $k = \infty$, we get as uncertainty set $\mathcal{U}_\infty = \{\phi \in \mathbb{R}^{N_\phi} \mid \underline{\phi} \leq \phi \leq \overline{\phi}\}$.*

In the next step we want to formulate the optimization problem in such a way that is robust with respect to changes in the uncertain parameter ϕ. For this we choose the worst-case formulation [8, 12, 44]. With this approach we incorporate the uncertainty into the nominal optimization problem (14). We define the *worst-case function* as

$$\varphi_i(p) := \max_{\phi \in \mathcal{U}_k} g_i(p; \phi), \quad i = 0, \ldots, N_g.$$

The function $\varphi_i : \mathcal{U}_k \to \mathbb{R}$ gives for every fixed parameter p the worst-case value of the function g_i under the condition that ϕ lies in the uncertainty set. Using the definition of the uncertainty set, the worst-case function can be rewritten as

$$\varphi_i(p) := \max_{\phi \in \mathbb{R}^{N_\phi}} g_i(p; \phi) \quad \text{subject to} \quad \|D^{-1}(\phi - \hat{\phi})\|_k \leq 1, \quad i = 0, \ldots, N_g.$$

Using this function we can now formulate the robust version of (14) as

$$\min_{p \in \mathbb{R}^{N_p}} \varphi_0(p) \quad \text{s.t.} \quad \varphi_i(p) \leq 0, \quad i = 1, \ldots, N_g. \tag{16}$$

This problem is referred to as the *robust counterpart* of (14). A solution p that satisfies (16) is referred to as *robust optimal solution*. This optimal solution is robust against uncertainty since it is feasible for (14) no matter which $\phi \in \mathcal{U}_k$ is chosen, and optimal with respect to the objective function g_0.

The robust optimization problem (16) is difficult to solve due to its bi-level structure. This has been investigated in [7] for a variety of problems. In [8] for general nonlinear problems it was proposed to replace the robust counterpart (16) by an approximation

$$\min_{p \in \mathbb{R}^{N_p}} \hat{\varphi}_0(p) \quad \text{subject to} \quad \hat{\varphi}_i(p) \leq 0, \quad i = 1, \ldots, N_g, \tag{17}$$

where the *approximated worst-case function* $\hat{\varphi}_i$ can be computed more efficiently compared to the original worst-case function φ_i. The new problem is then referred to as the *approximated robust counterpart* of (14).

In the following we investigate first and second order approximations of φ_i. While the first order approximation has already been investigated for the general nonlinear case in [12, 44], the quadratic approximation is new. The second order approximation utilized in this work is a modification of the approach presented in [38].

3.2.1. Linear approximation of the robust counterpart

Let us recall the suggested approach of [12, 44] and rewrite it using the introduced notation. The linearization is carried out around a nominal value

$\hat{\phi}$ of the uncertain parameter. Hence, we get for the approximated worst-case function

$$\hat{\varphi}_i(p) := \max_{\delta_i \in \mathbb{R}^{N_\phi}} g_i(p; \hat{\phi}) + \nabla_\phi g_i(p; \hat{\phi})\delta_i \quad \text{s.t.} \quad \|D^{-1}\delta_i\|_k \leq 1,\ i = 0, \dots, N_g.$$

This convex optimization problem can now be solved analytically and the solution is given by

$$\hat{\varphi}_i(p) = g_i(p; \hat{\phi}) + \|D\nabla_\phi g_i(p; \hat{\phi})\|_{k^*},$$

where $\|D \cdot \|_{k^*}$ is the dual norm of $\|D^{-1} \cdot \|_k$ with $k^* = k/(k-1)$ and we define $k^* = 1$ for $k = \infty$. Note that this is a standard result for scaled Hölder norms. Utilizing these results the linear approximated robust counterpart reads as

$$\min_{p \in \mathbb{R}^{N_p}} g_0(p; \hat{\phi}) + \|D\nabla_\phi g_0(p; \hat{\phi})\|_{k^*}$$

$$\text{s.t. } g_i(p; \hat{\phi}) + \|D\nabla_\phi g_i(p; \hat{\phi})\|_{k^*} \leq 0, \quad i = 1, \dots, N_g. \tag{18}$$

Problem (18) is the linear robust approximation of the nominal optimization problem (14). Note that the objective function and the inequality constraints are nondifferentiable if the term inside the norm becomes zero. For the case $k = \infty$ this can be circumvented by introducing slack variables, i.e.,

$$\min_{p \in \mathbb{R}^{N_p}, \zeta_i \in \mathbb{R}} g_0(p; \hat{\phi}) + \zeta_0 \quad \text{s.t.} \quad g_i(p; \hat{\phi}) + \zeta_i \leq 0, \quad i = 1, \dots, N_g,$$

$$-\zeta_i \leq D\nabla_\phi g_i(p; \hat{\phi}) \leq \zeta_i, \quad i = 0, \dots, N_g.$$

For $k = 2$ there is no such reformulation. Since there are only very few points, where this occurs there is a reasonable hope that standard algorithms for smooth nonlinear problems might work without any modification. Nevertheless one has to verify that the robust optimal solution does not lie in a nondifferentiable point [12, 38].

The computation of the derivatives can be carried out using either the adjoint approach or the sensitivity approach [20]. For a detailed discussion about the different approaches we refer the reader to [12].

3.2.2. Quadratic approximation of the robust counterpart

The first order approach is numerically very efficient but can suffer from an inaccurate approximation. Hence the influence of the uncertain parameter ϕ might be described insufficiently. This was already observed in [13]. Therefore, we seek for a higher order approximation. This approach was already investigated in [38], where the objective function and inequality constraints are approximated by quadratic Taylor expansions while the PDE constraint is linearized. In the presented work the PDE constraint is eliminated in (13) by introducing the reduced problem (14). By applying the second order approximation to (14) we implicitly apply the higher order approximation to the PDE constraint. This strategy was recently investigated in [28]. Next we outline the

construction of the robust counterpart. First we introduce the second order Taylor expansion of the worst-case function:

$$\hat{\varphi}_i(p) := \max_{\delta_i \in \mathbb{R}^{N_\phi}} g_i(p; \hat{\phi}) + \nabla_\phi g_i(p; \hat{\phi})\delta_i + \frac{1}{2}\delta_i^\top H_i(p; \hat{\phi})\delta_i$$

$$\text{s.t.} \quad \|D^{-1}\delta_i\|_k \leq 1, \ i = 0, \ldots, N_g, \tag{19}$$

where H_i is a symmetric approximation on $\nabla_{\phi\phi}g_i(p; \hat{\phi})$. Compared to the first order approximation, it is not possible to write down a closed form expression for $\hat{\varphi}_i(p)$. However, the quadratic approximation of the worst-case function corresponds to a trust region problem with $k = 2$. For these problems, exact solutions can be characterized by the following theorem [11, 20].

Theorem 3.1. *The trust region problem* (19) *possesses a global solution* δ_i *if and only if there exists a Lagrange multiplier* λ_i *satisfying*

$$(-H_i(\cdot, \hat{\phi}) + \lambda_i \mathbb{D})\delta_i = \nabla_\phi g_i(\cdot, \hat{\phi}), \quad \lambda_i(\|D^{-1}\delta_i\|_2 - 1) = 0, \quad \lambda_i \geq 0, \quad \|D^{-1}\delta_i\|_2 \leq 1$$

and $-H(\cdot, \hat{\phi}) + \lambda_i \mathbb{D}$ *positive semidefinite with* $\mathbb{D} = D^{-\top}D^{-1}$.

By adding a square to the norms in the constraints we relax the problem and obtain the differentiable formulation of the quadratic approximation of the robust counterpart

$$\min_{p \in \mathbb{R}^{N_P}, \delta_0, \ldots, \delta_{N_g} \in \mathbb{R}^{N_\phi}, \lambda_0, \ldots, \lambda_{N_g} \in \mathbb{R}} g_0(p; \hat{\phi}) + \nabla_\phi g_0(p; \hat{\phi})\delta_0 + \frac{1}{2}\delta_0^\top \nabla_{\phi\phi}g_0(p; \hat{\phi})\delta_0$$

$$\text{s.t.} \quad g_i(p; \hat{\phi}) + \nabla_\phi g_i(p; \hat{\phi})\delta_i + \frac{1}{2}\delta_i^\top \nabla_{\phi\phi}g_i(p; \hat{\phi})\delta_i \leq 0, \quad i = 1, \ldots, N_g,$$

$$\begin{pmatrix} -\nabla_\phi g_i(\cdot, \hat{\phi}) - \nabla_{\phi\phi}g_i(\cdot, \hat{\phi})\delta_i + \lambda_i \mathbb{D}\delta_i \\ \lambda_i(\|D^{-1}\delta_i\|_2^2 - 1) \end{pmatrix} = 0, \quad i = 0, \ldots, N_g,$$

$$\|D^{-1}\delta_i\|_2^2 - 1 \leq 0, \quad i = 0, \ldots, N_g,$$

$$-\lambda_i \leq 0, \quad i = 0, \ldots, N_g,$$

$$\nabla_{\phi\phi}g_i(\cdot, \hat{\phi}) - \lambda_i \mathbb{D} \preceq 0, \quad i = 0, \ldots, N_g, \tag{20}$$

where $A \preceq 0$ denotes that A is a negative definite matrix. The semidefinite constraint can be reformulated using the smallest eigenvalues. This approach was outlined in [38]. Note that (20) is a *mathematical program with equilibrium constraints* (MPEC). This type of problem can be solved efficiently by a SQP method under relatively mild assumptions [16, 29]. The required derivatives for the quadratic approximation can again be derived in different ways. In this work we assume that the number of parameters is small and we opted for a sensitivity based approach.

4. Proper Orthogonal Decomposition for Parametrized problems

Numerical approximation for robust optimization problems can be expensive since it involves the solution of several PDEs. Moreover, the sensitivity approach

enlarge the number of PDEs and it increases the computational costs of its approximation. For this reason, in this section, we introduce a model order reduction technique in order to reduce the complexity of the problem.

Here, we focus on the Proper Orthogonal Decomposition (POD) method for the approximate solution of the parametrized equation (9). In what follows $\mathbf{u}_h(p) \in \mathbb{R}^N$ is the model vector associated to the FE solution of (9) for a given parameter $p \in M_{ad} \subset \mathbb{R}^{N_p}$. For this purpose let $\{p^j\}_{j=1}^n$ be a grid in M_{ad} and let $\mathbf{u}_h(p^j)$ denote the corresponding solutions to (9) for the grid points p^j. We define the snapshots set $\mathcal{V} := \text{span}\{\mathbf{u}_h(p^1), \ldots, \mathbf{u}_h(p^n)\}$ and determine a POD basis $\mathcal{V}^\ell := \text{span}\{\psi_1, \ldots, \psi_\ell\}$ of rank ℓ by solving the following minimization problem:

$$\min_{\psi_1, \ldots, \psi_\ell} \sum_{j=1}^n \beta_j \left\| \mathbf{u}_h(p^j) - \sum_{i=1}^\ell \langle \mathbf{u}_h(p^j), \psi_i \rangle_\mathbf{W} \psi_i \right\|_\mathbf{W}^2$$
$$\text{s.t.} \langle \psi_j, \psi_i \rangle_\mathbf{W} = \delta_{ij} \quad \text{for } 1 \le i, j \le \ell, \tag{21}$$

where β_j are nonnegative weights, δ_{ij} denotes the Kronecker symbol, $\mathbf{W}$ is a symmetric positive definite $N \times N$ matrix and $\psi_i \in \mathbb{R}^n$. The weighted inner product used is defined as follows: $\langle \mathbf{u}, \mathbf{v} \rangle_W := \mathbf{u}^\top \mathbf{W} \mathbf{v}$.

It is well-known (see [17]) that problem (21) admits a unique solution $\{\psi_1, \ldots, \psi_\ell\}$, where ψ_i denotes the i−th eigenvector of the self-adjoint linear operator $\mathcal{R}$: $\mathbb{R}^n \to \mathbb{R}^n$, i.e., $\mathcal{R}\psi_i = \lambda_i \psi_i$ with $\lambda_i \in \mathbb{R}^N$ non-negative, where $\mathcal{R}$ is defined as:

$$\mathcal{R}\psi = \sum_{j=1}^n \beta_j \langle \mathbf{u}_h(p^j), \psi \rangle_\mathbf{W} \mathbf{u}_h(p^j) \quad \text{for } \psi \in \mathbb{R}^n.$$

Moreover the error in (21) can be expressed as follows:

$$\sum_{j=1}^n \alpha_j \left\| \mathbf{u}_h(p^j) - \sum_{i=1}^\ell \langle \mathbf{u}_h(p^j), \psi_i \rangle_\mathbf{W} \psi_i \right\|_\mathbf{W}^2 = \sum_{i=\ell+1}^d \lambda_i. \tag{22}$$

4.1. POD approximation for state and sensitivities

We briefly recall how to generate the reduced order modeling by means of POD. Suppose we have computed the POD basis $\{\psi_i, \ldots, \psi_\ell\}$ of rank ℓ according to the minimization problem (21). For the weight matrix we choose

$$\mathbf{W} := \mathbf{K}(\bar{p}) + \mathbf{M}(\bar{p}),$$

where $\bar{p}$ is a fixed reference parameter and $\mathbf{M}$ denotes the mass matrix. Then, $\mathbf{W}$ is the matrix associated to the discrete H^1−norm. We define the POD ansatz for the state as $\mathbf{u}_h^\ell(p) := \sum_{i=1}^\ell (\bar{\mathbf{u}}^\ell)_i \psi_i$. This ansatz in (9) leads to an ℓ−dimensional linear system for the unknown $\{\bar{\mathbf{u}}_i\}_{i=1}^\ell$, namely

$$\mathbf{K}^\ell(p)\bar{\mathbf{u}}(p) = \mathbf{f}^\ell(p). \tag{23}$$

11

Here the entries of the stiffness matrix are given by $(\mathbf{K}^\ell)_{ij} = \psi_i^\top \mathbf{K}(p)\psi_j$ for $1 \leq i, j \leq \ell$. The right hand side is given by $(\mathbf{f}^\ell)_i = \psi_i^\top \mathbf{f}(p)$, $1 \leq i \leq \ell$. We recall that due to the previously introduced affine decomposition this projection has to be computed only once and the system matrix can be written as

$$\mathbf{K}^\ell(p) = \sum_{q=1}^{Q} \Theta_a^q(p)\mathbf{K}^{q,\ell},$$

where $(\mathbf{K}^{q,\ell})_{ij} = \psi_i^\top \mathbf{K}^q \psi_j$ for $1 \leq i, j \leq \ell$ and $q = 1, \ldots, Q$. The same structure can be used for the right hand side. Note that this is very important in order to obtain an efficient reduced order model since the system can be set up for different values of p without the need of the original high dimensional matrices and right hand sides. The reduced order state equation reads:

$$\begin{cases} \text{For } p \in \mathcal{D} \text{ find } \mathbf{u}_h^\ell \in \mathcal{V}^\ell \text{ s.t.} \\ \mathbf{K}^\ell(p)\mathbf{u}_h^\ell(p) = \mathbf{f}^\ell(p). \end{cases} \tag{24}$$

In an analogous way we obtain the general reduced sensitivity equation from (12). We need to make an ansatz for the sensitivities $\mathbf{u}_{h,i}^{n,\ell}$ and project the system onto the subspace spanned by the POD basis. Note that in the present work we use the same basis functions for the state and the sensitivities variables. A better approximation property might be achieved by adding the solution of the sensitivity equation to the snapshots set. Note that in the reduced sensitivity equation the stiffness matrix is the same as in the reduced state equation, so that only the right-hand side needs to be projected.

4.2. A-posteriori error estimations

A-posteriori error estimators have a crucial role in model order reduction. They provide a certification of the surrogate model without the need of the computation of the truth solution. In the present work, we consider as truth solution the finite element approximation. A lower bound for the coercivity constant $\alpha(p)$ in (4) is computed following the $\min-\Theta$ theorem introduced in [34]. It turns out that

$$\alpha_{LB}(p) := \min_q \frac{\Theta_a^q(p)}{\Theta_a^q(\bar{p})} < \alpha(p),$$

where $\bar{p}$ is the fixed reference parameter. An upper bound for the continuity constant $\gamma(p)$ in (5) is given by

$$\gamma(p) < \gamma_{UB}(p) := \max_q \frac{\Theta_a^q(p)}{\Theta_a^q(\bar{p})}.$$

For more details we refer the reader to [34]. Then, we can derive an error bound for the reduced state and sensitivity equations (see [36] for more details) in terms of the reduced residual of the aforementioned equations. For this purpose let us define the residuals for equation (8) and (6) as

$$r_u(v; p) := f(v; p) - a(u_h^\ell, v; p) \quad \forall v \in X_h, p \in \mathcal{D}, \tag{25}$$

$$r_{u^1,i}(v;p) := f_i^1(v;p) - a_i^1(u_h^\ell, v:p) - a(u_{h,i}^{\ell,1}, v;p) \quad \forall v \in X_h, p \in \mathcal{D}, \qquad (26)$$

where $u_h^\ell = \sum_{i=1}^N (\mathbf{u}_h^\ell)_i \varphi_i$. Then, we have

Theorem 4.1. *Let $u_h \in X_h$ be the solution to (9) and $u_h^\ell \in X_h$ be the corresponding reduced solution of (23). Then, the error satisfies*

$$\|u_h - u_h^\ell\|_{X_h} \leq \Delta_u^\ell := \frac{\|r_u(\cdot,p)\|_{(X_h)'}}{\alpha(p)} \qquad (27)$$

where the dual norm is defined as $\|r_u(\cdot;p)\|_{(X_h)'} \equiv \sup_{v \in Y \backslash 0} \frac{|r_u(v;p)|}{\|v\|_{X_h}}$.

Proof. It follows from (9) and the definition of the residual $r_u(v;p)$ that the POD error, $u_h - u_h^\ell$ satisfies

$$a(u_h - u_h^\ell, v;p) = f(v;p) - a(u_h^\ell, v;p) = r_u(v;p) \quad \forall v \in X_h(\bar\Omega). \qquad (28)$$

Choosing $v = u_h - u_h^\ell$ in (28), invoking (4), and the dual norm of the residual we obtain

$$\alpha(p)\|u_h - u_h^\ell\|_{X_h}^2 \leq a(u_h - u_h^\ell, u_h - u_h^\ell; p) \leq \|r_u(\cdot,p)\|_{(X_h)'}\|u_h - u_h^\ell\|_{X_h},$$

from which the result directly follows.□

Next theorem addresses the a-posteriori error for the first sensitivity equation (11). For time dependent problems this has been shown in [14]. We recall the result for our particular setting and provide a short proof.

Theorem 4.2. *Let $u_h \in X_h$ be the solution to (9) and $u_h^\ell \in X_h$ be the corresponding reduced solution of (23). Further, let $u_h^1 \in X_h$ be the solution to (11) and $u_h^{1,\ell} \in X_h$ be the solution of the reduced sensitivity equations. Then, the inequality*

$$\|u_{h,i}^1 - u_{h,i}^{1,\ell}\|_{X_h} \leq \Delta_{u^1,i}^\ell(p) := \frac{1}{\alpha(p)}\left(\|r_{u^1,i}\|_{(X_h)'} + \gamma_{p_i}(p)\Delta_u^\ell(p)\right) \qquad (29)$$

with $\gamma_{p_i}(p) = \frac{\partial\gamma}{\partial p_i}(p)$ holds.

Proof. We denote the error of the state equation by $e_u := u_h - u_h^\ell$. It follows from the linearity of the sensitivity equations (6) that the error $e_{u^1,i} := u_{h,i}^1 - u_{h,i}^{1,\ell}$ satisfies:

$$
\begin{aligned}
a(e_{u^1,i}, v;p) &= a(u_{h,i}^1, v;p) - a(u_{h,i}^{1,\ell}, v;p) \\
&= f_i^1(v;p) - a_i^1(u_h, v;p) - a(u_{h,i}^{1,\ell}, v;p) + a_i^1(u_h^\ell, v;p) - a_i^1(u_h^\ell, v;p) \\
&= r_{u^1,i}(v;p) + a_i^1(u_h^\ell - u_h, v;p)
\end{aligned}
$$

Let us now test choosing $v = e_{u_h^1}(p)$. Then,

$$
\begin{aligned}
\alpha(p)\|e_{u^1,i}\|_{X_h}^2 &\leq a(e_{u^1,i}, e_{u_h^1}; p) = r_{u^1,i}(e_{u^1}; p) + a_i^1(u_h^\ell - u_h, e_{u^1,i}; p) \\
&\leq \|r_{u^1,i}(\cdot;p)\|_{(X_h)'}\|e_{u^1}\|_{X_h} + \gamma_p(p)\|u_h^\ell - u_h\|_{X_h}\|e_{u^1,i}\|_{X_h}
\end{aligned}
$$

holds. By using (27) for the term $\|u_h^\ell - u_h\|_{X_h}$ the result follows directly. □

13

General error estimate. The a-posteriori error estimates discussed in the previous subsection can be generalized to the $n-th$ sensitivity equation (12). To provide the associated result we for the ease of notation again assume $p \in \mathbb{R}$ and omit the index i.

Definition 4.3. *Let $u_h^{k,\ell} \in X_h$, $k = 0, \ldots, n$ be the reduced order solution of (12). We define the residual:*

$$r_{u^n}(v;p) := f^n(v;p) - \sum_{k=1}^{n} \binom{n}{k} a^k(u_h^{n-k,\ell}, v; p) - a(u_h^{n,\ell}, v; p) \qquad (30)$$

We note that for $n = 0$ and $n = 1$ we find the state and sensitivity residual (25) and (26) Then, we have

Theorem 4.4. *Let $u_h^n \in X_h$ be the solution to (12) and $u_h^{n,\ell} \in X_h$ be the corresponding reduced solution of (12). Then, the following inequality holds:*

$$\|u_h^n - u_h^{n,\ell}\|_{X_h} \leq \Delta_{u^n}^{\ell}(p) := \frac{1}{\alpha(p)} \left(\|r_{u^n}\|_{(X_h)'}| + \sum_{k=1}^{n} \binom{n}{k} \gamma_k \Delta_{u^{n-k}}^{\ell} \right), \qquad (31)$$

where γ_k is the continuity constant of the k-th derivative of the coercive bilinear form.

Proof. We denote the error by $e_{u^n} := u_h^n - u_h^{n,\ell}$. With (7) we find that

$$
\begin{aligned}
a(e_{u_h^n}, v; p) &= a(u_h^n, v; p) - a(u_h^{n,\ell}, v; p) \\
&= f^n(v;p) - \sum_{k=1}^{n} \binom{n}{k} a^k(u_h^{n-k}, v; p) - a(u_h^{n,\ell}, v; p) \\
&\quad + \sum_{k=1}^{n} \binom{n}{k} a^k(u_h^{n-k,\ell}, v; p) - \sum_{k=1}^{n} \binom{n}{k} a^k(u_h^{n-k,\ell}, v; p) \\
&= r_{u^n}(v;p) + \sum_{k=1}^{n} \binom{n}{k} a^k(u_h^{n-k,\ell} - u_h^{n-k}, v; p)
\end{aligned}
$$

Now we set $v = e_{u^n}$ and obtain

$$a(e_{u_h^n}, e_{u_h^n}; p) = r_{u^n}(e_{u_h^n}; p) + \sum_{k=1}^{n} \binom{n}{k} a^k(u_h^{n-k,\ell} - u_h^{n-k}, e_{u_h^n}; p)$$

By applying Cauchy-Schwarz and using the coercivity of a as well as the continuity of a^k we find

$$\alpha(p)\|e_{u_h^n}\|_{X_h}^2 \leq \|r_{u^n}(\cdot; p)\|_{(X_h)'}\|e_{u_h^n}\|_{X_h} + \sum_{k=1}^{n} \binom{n}{k} \gamma_k \|u_h^{n-k,\ell} - u_h^{n-k}\|_{X_h}\|e_{u_h^n}\|_{X_h}$$

Bounding $\|u_h^{n-k,\ell} - u_h^{n-k}\|_{X_h} \leq \Delta_{u^{n-k}}^{\ell}$ and dividing by $\alpha(p)\|e_{u_h^n}\|_{X_h}$ leads to (31). $\square$

14

Remark 4.1. *We note that* (31) *is a generalization of the error bounds for state and first order sensitivity equations. In fact for $n = 0$ we obtain* (27)*, and for $n = 1$* (29)*.*

Remark 4.2. *The presented generalized error estimator* (31) *is not limited to the introduced setting arising from a parametrized shape optimization. In fact, if only the linear form f depends on the parameter p, i.e., $a(u, v) = f(v; p)$, the error estimator reads*

$$\|u_h^n - u_h^{n,\ell}\|_{X_h} \leq \frac{\|r_{u^n}\|_{(X_h)'}}{\alpha}.$$

4.3. The POD method for optimization problem

In this section we explain how to solve the reduced optimal control problem. To build the reduced order model we have to select some relevant parameters related to the optimal control problem. The snapshot set is important for POD model reduction, since the basis functions are built upon this set. Therefore, the choice of the parameters should be done according to our optimal control problem. For this reason we propose a goal-oriented algorithm for the computation of the POD basis functions. The goal is given by the error bound $\Delta_{u^n}^\ell$ for state and sensitivity introduced in Section 4.2. This error indicator helps also in the selection of the snapshots set. The algorithm works as follows: we start with a very coarse parameter sample choosing only one parameter p^0 and solve the full problem together with the sensitivity equations associated to this parameter. Then we compute the POD basis functions and perform the reduced optimization procedure. At the end of the process we find a new parameter p^1 which is an approximation of the optimal desired design, we update the parameter set $\mathcal{D} = \{p^0, p^1\} \subset M_{ad}$, solve the full problem and the sensitivity equations related to the new parameter p^1. Then, we enlarge the snapshots set and compute new POD basis functions. We iterate this process until the stopping criteria is reached.

The procedure is summarized in Algorithm 1.

Algorithm 1 (Goal-Oriented POD optimization)

Require: $p^0, \mathbf{u}^0(p^0), \mathcal{V} = [], k = 0, tol > 0$

  1: **while** $\Delta_{u^i}^\ell \leq tol$ **do**

  2:     Compute sensitivities $\mathbf{u}^i(p^k)$, for $i = 1, 2, 3, \dots N_p$

  3:     Set Snapshot set

$$\mathcal{V} = [\mathcal{V}, \mathbf{u}^0(p^k), \mathbf{u}^1(p^k), \mathbf{u}^2(p^k), \mathbf{u}^3(p^k), \dots \mathbf{u}^{N_p}(p^k)]$$

  4:     Compute POD basis functions $\{\psi_i\}_{i=1}^\ell$ with $\ell = \text{rank}(\mathcal{V})$

  5:     Find p^{k+1} solving the OCP with the reduced order modeling (24)

  6:     Compute $\mathbf{u}^{i,\ell}(p^{k+1})$ and $\mathbf{u}^i(p^{k+1})$,

  7:     Set k=k+1

  8: **end while**

In our simulations this approach turned out to be very efficient since it avoids long pre-computations. In this way we are able to update the snapshot set and the POD basis functions. Our update contains information on the optimal control problem and it improves the quality of our surrogate model. Note that every reduced optimization problem contains the a-posteriori error for the state and sensitivity equations introduced in Section 4.2. In this way we update the snapshot set, and therefore the POD basis, not only when we are close to the minimum of the problem, but even if the reduced model is not accurate enough. However, our update contains information on the optimal control problem and it improves the quality of our surrogate model.

5. Numerical tests

In our numerical example we consider an optimal design problem for a permanent magnet synchronous machine. We start by introducing the model and geometry under consideration. We consider a three-phase six-pole permanent magnet synchronous machine (PMSM) with one buried permanent magnet per pole. The geometry is shown in Figure 1. The goal of the design optimization is to change the size and location of the permanent magnet such that the material of the magnet is minimized while maintaining the electromotive force. We consider a description using three parameters: p_1 the width, p_2 the height and p_3 the central perpendicular distance between the rotor and the surface of the magnet. The region around the permanent magnet (Figure 1 red box) is decomposed into twelve triangles (Figure 1 blue lines). The introduced triangulation of the parametrized domain allows to perform the affine linear decomposition as introduced in (10) with $Q = 12$.

PMSMs can be described sufficiently accurate by the magnetostatic approximation of Maxwell's equation. In the governing parametrized equation is given by

$$\nabla \times (\nu(p)\nabla \times u(p)) = J_{src}(p) - \nabla \times H_{pm}(p), \tag{32}$$

with boundary conditions

$$u|_{BC} = u|_{DA} = 0 \quad \text{and} \quad u|_{AB} = -u|_{CD}$$

where ν is the reluctivity, J_{src} is the source current density and H_{pm} the field of the permanent magnets (PM). In the 2D planar setting and using the finite element method for the magnetic vector potential, this leads to the discrete form given by the linear model presented in (9). To extract performance values the loading method is used which exploits the frequency domain [35]. To obtain quantities like the electromotive force (EMF) a Fourier analysis of the magnetic vector potential around the inner surface of the stator is carried out. This can be written as a linear function $E_0 = l(\mathbf{u}_h; p) = \mathbb{E}^\top \mathbf{u}_h$. More details on the configuration we adopt in the present work can be found in [2, 22, 33].

Let us next formulate the optimization problem. We start by introducing the nominal optimization problem. The goal of the optimization is to minimize
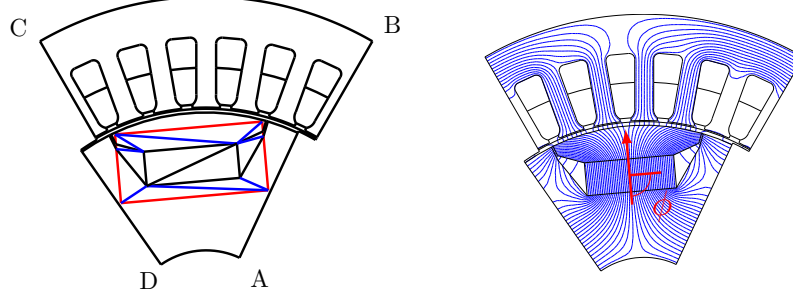
Figure 1: Geometry configuration with region for the affine decomposition (red box) and triangulation for the decomposition (blue lines) (left plot). Magnetic vector potential for the geometry configuration and magnetic field angle ϕ (right plot).

the required material for the permanent magnet while maintaining the EMF E_0. In the mathematical model this leads to a cost function of the form

$$\min_{p \in \mathbb{R}^3} g_0(p) := p_1 p_2 + \rho \max(0, E_0^d - E_0(p, \mathbf{u}(p))),$$

where E_0^d is the desired EMF and $\rho \in \mathbb{R}^+$ a weight parameter. Additionally, we have the constraints

$$(1,1,5) \leq (p_1, p_2, p_3) \leq (\infty, \infty, 14), \quad p_2 + p_3 \leq 15 \quad \text{and} \quad 3p_1 - 2p_3 \leq 50.$$

The upper and lower bounds for the parameters and the first inequality are due to the parametrization of the geometry and the restriction that the permanent magnet has to stay within the red box in Figure 1 (left). The last inequality is a design restriction that avoids that the corner of the permanent magnet comes too close to the rotor surface. Note that we right away use the reduced formulation as introduced in (14). To obtain a smooth formulation we introduce a slack variable. We reformulate the nominal optimization problem by using the variable $x = (p, \xi)$ as

$$\min_{x \in \mathbb{R}^4} g_0(x) := p_1 p_2 + \rho \xi \quad \text{s.t.} \quad g_{1,\ldots,8}(x) = \begin{pmatrix} p_2 + p_3 - 15 \\ 3p_1 - 2p_3 - 50 \\ E_0^d - E_0(\mathbf{u}_h, p) - \xi \\ 1 - p_1 \\ 1 - p_2 \\ 5 - p_3 \\ -\xi \\ p_3 - 14 \end{pmatrix} \leq 0. \quad (33)$$

In this form the optimization problem fits exactly into the framework of (14).

Next let us introduce the uncertainty. For our numerical example we assume that the magnetic field angle in the permanent magnet is uncertain [31]. This

can be due to manufacturing imprecision. In the nominal optimization the magnetic field is aligned perfectly, i.e. the field angle is 90°, see Figure 1 (right plot). In practice this can not be met and a deviation is to be expected. The field angle enters the model problem (32) nonlinearly through the right hand side, in particular in the term H_{pm}. In our numerical example we allow a field angle ϕ in the range $[80°, 90°]$. Following the definition of the uncertainty set in Section 3.2 we get

$$\mathcal{U}_k = \left\{ \phi \in \mathbb{R} \,\middle|\, \phi = 85 + \delta, \, \|0.2\delta\|_k \leq 1 \right\}$$

with $k \in \{2, \infty\}$, i.e. $\hat{\phi} = 85$ and $D = 5$ in (15). Using this settings we can now solve the linear and quadratic approximation of the robust counterpart (18) and (20). In the case of the linear approximation we choose $k = \infty$ and for the quadratic approximation we set $k = 2$.

Before presenting the numerical results let us give a short overview of the numerical strategy utilized to solve the optimization problems. The computations are carried out in MATLAB. To solve the nominal and robust optimization problems an SQP method with Armijo-backtracking strategy using a ℓ_1-penalty function is used [30]. The Hessian is computed via BFGS updates. Alternatively also routines like `fmincon` in MATLAB can be used obtaining similar results. The derivative of g_i, $i = 0, \ldots, 8$ are computed using the sensitivity approach [20]. Also the derivatives with respect to the uncertain parameter ϕ are computed using this approach. The structure of the sensitivity equations are as outlined in (11).

5.1. Results obtained by the finite element approximation

We start by presenting the numerical results utilizing the finite element approximation. Piecewise linear and continuous finite elements are used to discretize equation (32) leading to a system with 61013 degrees of freedom.

The initial geometry configuration corresponding to $p = (19, 7, 7)$ is shown in Figure 1 (left) together with the corresponding magnetic vector potential (right). From the magnetic vector potential we extract the EMF which we will use as the desired value $E_0^d = 30.72$ in our optimization problem.

In Table 1 we show the results obtained in the optimization. In column V_{pm} the volume of the permanent magnets is given. Note that through the optimization a significant reduction in size is achieved. The ratio is given in percent in the second column. For the nominal optimization a reduction by 53% is obtained and in the robust case reductions of 50% (linear case) and 49% (quadratic case). The respective parameters are given in the third column. Lastly, in column four and five the EMF E_0 for the field angle $\phi = 90°$ and the worst-case EMF E_0^{worst} are given. It can be seen that the uncertainty in the magnetic field of the permanent magnet has an impact on the performance. In the robust optimization this influence is incorporated. Hence it can be seen that in the case of the quadratic approximation very good results can be achieved. The worst-case EMF stays above the target value of 30.3702. In the case of the nominal optimization a significant decay can be observed. In the case of the

18

	V_{pm}	%	p	E_0 (90°)	E_0^{worst}
Init	133.00	100	$(19.00, 7.00, 7.00)$	30.3483	29.8873
Nom. Opt	62.36	47	$(21.08, 2.96, 6.62)$	30.3483	29.8873
Rob. Lin	66.46	50	$(21.10, 3.15, 6.64)$	30.5817	30.2322
Rob. Quad	67.95	51	$(21.10, 3.22, 6.65)$	30.6995	30.3487

Table 1: Comparison of the results obtained by the optimization and robust optimization using different approximation orders.

linear approximation the target can not be met since the approximation is not accurate enough. It can also be observed that by performing only a nominal optimization the worst-case can decrease compared to the initial configuration. In the presented case the difference is small but can become more significant in different settings.

The approximation quality and the behaviour of the EMF is shown in Figure 2 for the different optimal designs. In the left plot the behaviour of the EMF for different permanent magnet field angles ϕ is shown for the initial and the nominal optimal configuration. It can be seen that the target E_0^d is only reached in $\phi = 90°$. In the middle plot the linear approximation and the actual EMF are compared. It can be seen that the approximation is not accurate enough to determine the worst-case. The right plot corresponds to the quadratic approximation. It can be seen that the EMF is approximated very well by the quadratic model. Hence also good results in the robust optimization using this approximation can be expected.
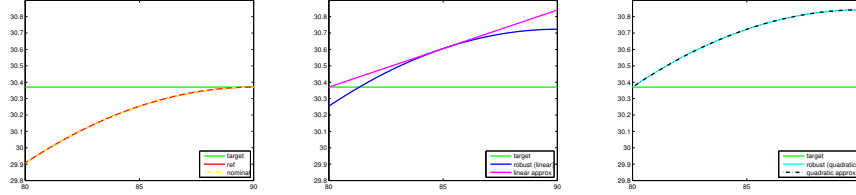

Figure 2: Influence of the permanent magnet field angle on the electromotive force for different geometry configuration.

Remark 5.1. *Note that our choice of the field angle ϕ in the range $[80°, 90°]$ has technical reasons. The EMF has an almost symmetric behaviour around the field angle of $90°$. Hence the linear approximation of the robust counterpart at around $\phi = 90°$ will fail since the derivative of g_i, $i = 0, \ldots, 8$, with respect to ϕ are almost zero. The quadratic approximation on the other hand has no problem in achieving a good approximation.*

In Figure 3 the magnetic vector potentials are shown for the three optimal designs. To conclude we have a look at the computational expenses for the optimization. These are summarized in Table 2, where the computational time
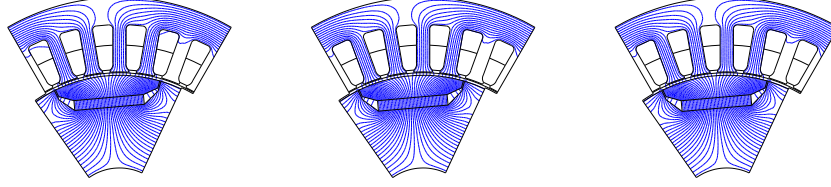
Figure 3: Magnetic vector potential for the geometry configuration obtained by the optimization. Nominal optimal design (left), robust optimal design with linear approximation (middle), and with quadratic approximation (right).

	CPU (s)	Iter	PDE solves
Nom. Opt	52.29	9	42
Rob. Lin	98.09	8	86
Rob. Quad	135.57	6	78

Table 2: Performance of the SQP method and computational cost.

in seconds, the number of iterations and the number of required PDE solves are compared. While the computational time in this example is still very low it can be seen that the robust optimization is more expensive. Especially the number of PDE solves increases significantly compared to the nominal optimization. Hence we will utilize model order reduction to reduce the computational costs. This will be outlined in the next section.

5.2. Results obtained by the reduced order model

Let us start our analysis of the reduced order model by dealing with the approximation of the state and the sensitiviy variables. To this aim we select 27 parameters chosen as follows:

$$\mathcal{D}_{train} = \{1, 10.5, 20\} \times \{1, 3, 5\} \times \{5, 7, 10\}$$

and we compute an enlarged snapshot set with state and sensitivities for each parameter in $\mathcal{D}_{train}$. Altogether, we collect 108 snapshots.

In Figure 4, we present an error analysis to check the quality of our a-posteriori error discussed in Section 4. We compare the error between the POD solution and the high dimensional approximation for state and sensitivities with the error bound presented in Section 4.2. With the $\mathbf{W}$-norm introduced in Section 4, we set

$$\mathcal{E}_n(p) := \max_{p \in \mathcal{D}_{test}} \|u_h^n(p) - u_h^{n,\ell}(p)\|_{\mathbf{W}}, \qquad n = 0, 1, 2, 3.$$

where $\mathcal{D}_{test}$ is chosen in the centers of the boxes of $\mathcal{D}_{train}$ as follows:

$$\mathcal{D}_{test} = \{5.75, 15.25\} \times \{2, 4\} \times \{6, 8.5\}.$$

20

As one can see model order reduction is able to reach only an error of size 10^{-3}. We also want to emphasize that a standard POD approach, with only 27 state snapshots in $\mathcal{D}_{train}$, is able to reach an accuracy of order 10^{-2} with 27 basis functions.
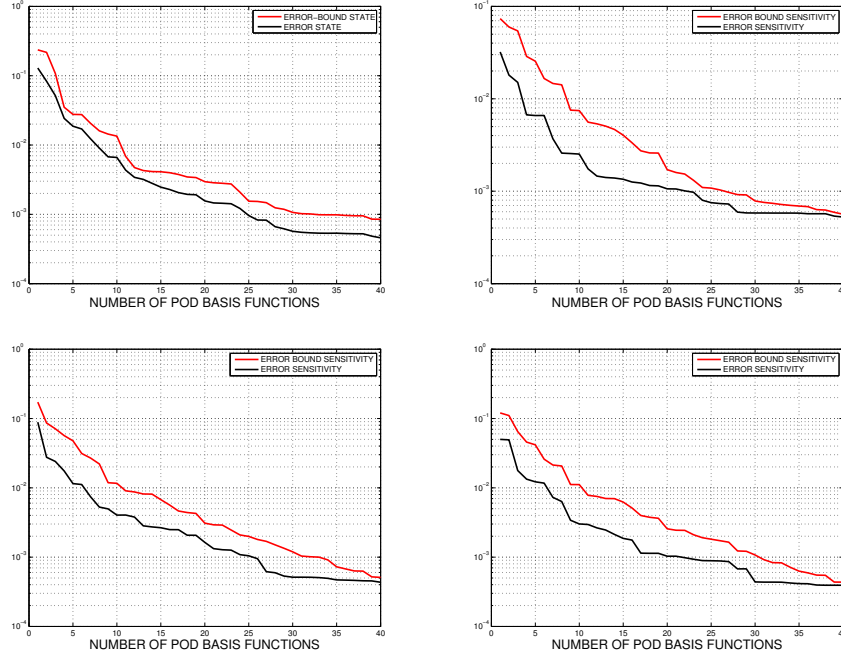

Figure 4: Maximum error over all parameter configurations related to $\mathcal{D}_{test}$. Error behavior $\mathcal{E}_0$ and error bound for state equation (top-left), Error behavior $\mathcal{E}_n$ for $n = 1, 2, 3$ and error bound for the sensitivity equations (top-right and bottom).

In Figure 5, we show it is possible to reach an accuracy of order 10^{-6} or higher with only 4 POD basis functions if we compute the snapshots with respect to one parameter in $\mathcal{D}_{train}$ and then compute the error in a neighborhood of the chosen parameter. This is our motivation to introduce Algorithms 1 for the successive enrichment of the POD model. In fact, we start our algorithm with only one parameter and we require the combined snapshots since in any other case we will not have enough data to generate a surrogate model from the simulation and the sensitivities. We note that if we add the sensitivities, the POD basis functions are improved and the parameter domain can better be explored. We refer the interested reader to [19] for more details.

Let us now draw our attention to the optimization problem and its performances when combined with model order reduction. Table 3 shows the convergence of Algorithm 1 for the nominal optimization. The number of updates of the snapshot set is given in the first column. Since our goal is to reach a desired electromotive force, we set as a stopping criteria the difference between
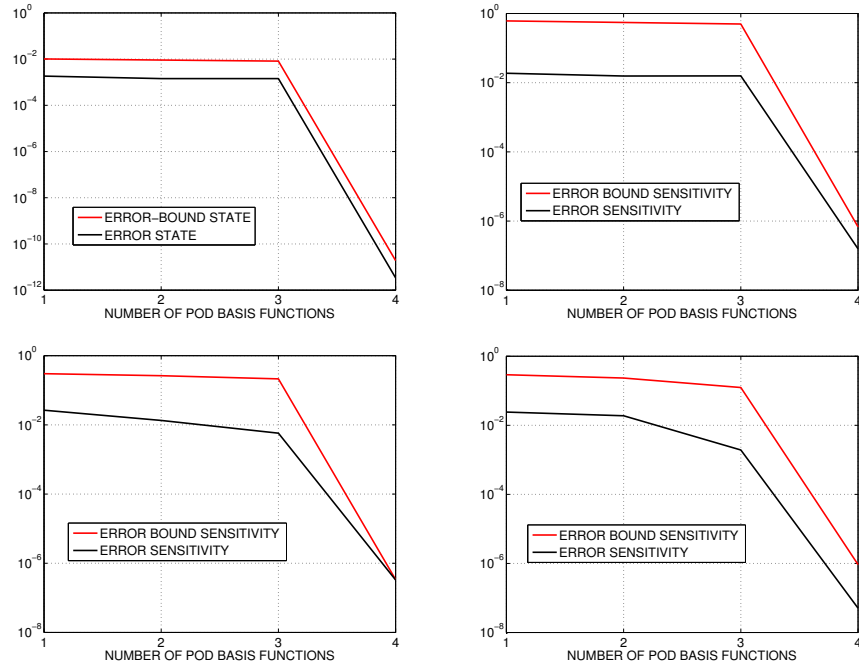
21

Figure 5: Maximum error of the surrogate model computed with respect to a parameter in the neighborhood of $\mathcal{D}_{train}$. Error behavior for state equation (top-left), and for the sensitivity equations for each parameter (top-right and bottom).

$E_0(p, \mathbf{u}_h^\ell(p), 90°)$ obtained from the POD, and $E_0(p, \mathbf{u}_h(p), 90°)$ obtained from the full simulaiton. Furthermore, we note that the electromotive force is a linear function which allows us to use the a-posteriori estimator for the state variable. As one can see we wIth the surrogate-based optimization obtain the same results as with the full model. The fifth column presents the number of iterations needed in each sub-optimization problem and the sixth column presents the error estimation of the state equation. In the stopping criterium of Algorithm 1 we choose $tol = 1e - 4$. In the last column we show the number of basis functions which also represents the dimension of the reduced problem. We note that the results of the algorithm are close to what we have shown in Table 2. The CPU time will be discussed at the end of the section.

iter	$E_0(p, \mathbf{u}_h(p), 90°)$	$E_0(p, \mathbf{u}_h^\ell(p), 90°)$	V	#it	Δ_u	ℓ
0	30.232855	30.232855	133.000000			
1	30.389505	30.348290	62.823870	8	5.24e-02	4
2	30.348284	30.348290	62.358918	4	1.49e-07	8

Table 3: Performance of POD with nominal optimization

Next we analyze the performance of POD for the robust optimization problem. In Table 4 we present the results of POD with a linear approximation of the robust counterpart. As one can see we obtain an impressive reduction of the amount of PDEs solved, keeping the same accuracy attained in the high dimensional problem (compare Table 6).

iter	$E_0(p, \mathbf{u}_h(p), 90°)$	$E_0(p, \mathbf{u}_h^\ell(p), 90°)$	V	#it	Δ_u	ℓ
0	30.232855	30.232855	133.000000			
1	30.512071	30.465362	67.364979	8	7.12e-02	8
2	30.465418	30.465425	65.045857	4	9.83e-06	16

Table 4: Performance of POD with linear robust optimization

In Table 5 we present the result within the surrogate model for the solution of the robust optimization problem with quadratic approximation. The same considerations discussed in the linear example hold true. We note that the number of POD basis functions used in each optimization in this case is larger due to a richer snapshot set.

iter	$E_0(p, \mathbf{u}_h(p), 90°)$	$E_0(p, \mathbf{u}_h^\ell(p), 90°)$	V	#it	Δ_u	ℓ
0	30.232855	30.232855	133.000000			
1	30.631991	30.582897	67.090115	6	6.73e-02	12
2	30.582764	30.582771	66.473438	5	5.14e-06	24

Table 5: Performance of POD with quadratic robust optimization

Also in the quadratic case we obtain the same approximation quality as in the full model at lower computational costs (give numbers here!). Moreover, the

presented numbers for both the linear and the quadratic case are in very good agreement of those presented in Table 1.

The computational costs of the POD approach are summarized in Table 6. Although we solve more (reduced) PDEs the CPU time is reduced significantly due to the number of full dimensional PDEs to be solved in the full setting, compare Tables 2 and 6). Finally, we note that the CPU time involves both offline and online stage, so that the speed up is effective.

	CPU (s)	Iter	PDE solves	Reduced PDE solves
Nom. Opt	22.5	12	8	48
Rob. Lin	29.3	11	24	110
Rob. Quad	39.9	11	36	132

Table 6: Performance of the POD method and computational cost.

6. Conclusion

In this paper we present a new approach which combines model order reduction to robust optimal control. We investigate an optimal control problem governed by a parametric elliptic partial differential equation with uncertain parameters. We introduce a robust optimization framework that accounts for uncertain model and optimization parameters. The resulting optimization problem, then, has a bi-level structure for the solution of this problem which leads to a non-linear optimization problem with a min-max formulation. We propose a goal-oriented model order reduction approach which avoids long offline stages and provides a certified reduced order surrogate model for the parametrized PDE which then is utilized in the numerical optimization. The presented numerical results clearly illustrate the validity and performance of the presented approach.

7. Acknowledgements

References

[1] K. Afanasiev and M. Hinze. *Adaptive control of a wake flow using proper orthogonal decomposition.* Lecture Notes in Pure and Applied Mathematics, **216**, 2001, 317-332.

[2] A. Alla, M. Hinze, O. Lass and S. Ulbrich. *Model order reduction approaches for the optimal design of permanent magnets in electro-magnetic machines.* In Proceedings of the MATHMOD 2015 - 8th Vienna International Conference on Mathematical Modelling.

[3] A. Alla and S. Volkwein. *Asymptotic stability of POD based model predictive control for a semilinear parabolic PDE.* Adv. Comput. Math. **41**, 2015, 1073-1102.

[4] A.C. Antoulas. Approximation of Large-Scale Dynamical Systems. SIAM, 2005.

[5] E. Arian, M. Fahl and E. Sachs. *Trust-region proper orthogonal decomposition models by optimization methods.* In Proceedings of the 41st IEEE Conference on Decision and Control, Las Vegas, Nevada, 2002, 3300-3305.

[6] J.A. Atwell and B.B. King. *Proper orthogonal decomposition for reduced basis feedback controllers for parabolic equations*, Matematical and Computer Modelling, **33**, 2001, 1-19.

[7] A. Ben-Tal, A. Goryashko and A. Nemirovski. *Robust optimization.* Princton University Press, 2009.

[8] A. Ben-Tal and A. Nemirovski. *Robust optimization – methodology and application.* Mathematical Programming, **92**, 2002, 453-480.

[9] D. Bertsimas, D.B. Brown and C. Caramanis. *Theory and application of robust optimization.* SIAM Review, **53**, 2011, 464–501.

[10] J. Birge and F. Louveaux. *Introduction to Stochastic Programming.* Springer, 1997.

[11] A.R. Conn, N.I.M. Gould and P.L. Toint. *Trust-Region Methods.* Society for Industrial and Applies Mathematics, 2000.

[12] M. Diehl, H.G. Bock and E. Kostina. *An approximation technique for robust nonlinear optimization.* Mathematical Programming, **107**, 2006, 213-230.

[13] M. Diehl, J. Gerhard, W. Marquardt and M. Mönnigmann. *Numerical solution approaches for robust nonlinear optimal control problems.* Computer & Chemical Engineering, **32**, 2008, 1287-1300.

[14] M. Dihlmann and B. Haasdonk. *Certified PDE-constrained parameter optimization using reduced basis surrogate models for evolution problems.* Computational Optimization and Applications, **60**, 2015, 753–787.

[15] L.C. Evans. *Partial Differential Equations.* American Math. Society, Providence, Rhode Island, 2008.

[16] R. Fletcher, S. Leyffer, D. Ralph and S. Scholtes. *Local convergance of SQP methods for mathematical programs with equilibrium constraints.* SIAM Journal on Optimization, **17**, 2006, 259-286.

[17] M. Gubisch and S. Volkwein. *Proper Orthogonal Decomposition for Linear-Quadratic Optimal Control.* To appear in P. Benner, A. Cohen, M. Ohlberger, and K. Willcox (eds.), Model Reduction and Approximation: Theory and Algorithms. SIAM, Philadelphia, PA, 2017.

[18] B. Haasdonk, and M. Ohlberger. Reduced Basis Method for Finite Volume Approximations of Parametrized Linear Evolution Equations. M2AN, Math. Model. Numer. Anal.,**42**, 2008, 277-302.

[19] A. Hay, J. Borggaard, D. Pelletier. *Local improvements to reduced-order models using sensitivity analysis of the proper orthogonal decomposition,* J. Fluid Mech. **629**, 2009, 41-72.

[20] M. Hinze, R. Pinnau, M. Ulbrich and S. Ulbrich. *Optimization with PDE Constraints. Mathematical Modelling: Theory and Applications, 23.* Springer Verlag, 2009.

[21] M. Hinze and S. Volkwein. *Proper orthogonal decomposition surrogate models for nonlinear dynamical systems: error estimates and suboptimal control*, in Reduction of Large-Scale Systems, P. Benner, V. Mehrmann, D. C. Sorensen (eds.), Lecture Notes in Computational Science and Engineering, **45**, 2005, 261-306.

[22] S. Hennerberger, U. Pahner, K. Hameyer and R. Belmans. *Computation of a highliy satured permanent magnet synchronous motor for a hybrid electric vehicle.* IEEE Trans. Magn., **33**, 1997, 4086-4088.

[23] B. Houska and M. Diehl. *Nonlinear robust optimization via sequential convex bilevel programming.* Mathematical Programming, **142**, 2013, 539–577.

[24] E. Kammann, F. Tröltzsch and S. Volkwein. *A method of a-posteriori error estimation with application to proper orthogonal decomposition.* ESAIM: M2AN, **47**, 2013, 555-581.

[25] M. K´archer and M. Grepl. *A certified reduced basis method for parametrized elliptic optimal control problems.* ESAIM: COCV, **20**, 416-441, 2014.

[26] D.P. Kouri and T.M. Surowiec. *Risk-averse PDE-constrained optimization using the conditional value-at-risk.* SIAM Journal on Optimization, **26**, 2016, 365–396.

[27] K. Kunisch, S. Volkwein, and L. Xie. *HJB-POD based feedback design for the optimal control of evolution problems*, SIAM J. on Applied Dynamical Systems, **4**, 2004, 701-722.

[28] O. Lass and S. Ulbrich. *Model order reduction techniques with a posteriori error control for nonlinear robust optimization governed by partial differential equations.* SIAM Journal on Scientific Computation, Accepted, 2017.

[29] S. Leyffer. *Complementarity constraints as nonlinear equations: Theory and numerical experience,* in Optimization with Multivalued Mappings: Theory, Applications, and Algo- rithms, S. Dempe and V. Kalashnikov (eds.), **2** of Springer Series in Optimization and Its Applications, Springer, 2006, 169-208.

[30] J. Nocedal and S.J. Wright. *Numerical Optimization, second edition.* Springer Series in Operation Research and Financial Engineering, 2006.

[31] P. Offermann and K. Hameyer. *A polynomial chaos meta-model for nonlinear stochastic magnet variations.* COMPEL - The international journal for computation and mathematics in electrical and electronic engineering, **32**, 2013, 1211–1218.

[32] B. Øksendal. *Optimal control of stochastic partial differential equations.* Stochastic Analysis and Applications, **23**, 2005, 165–179.

[33] U. Pahner. *A general design tool for terical optimization of electromagnetic energy transducers.* PhD Thesis, KU Leuven, 1998.

[34] A. T. Patera, G. Rozza. *Reduced Basis Approximation and A Posteriori Error Estimation for Parametrized Partial Differential Equations* MIT book, 2007.

[35] M.A. Rahman and P. Zhou. *Determination of saturated parameters of PM motors using loading magnetic fields.* IEEE Trans. Magn., **27**, 1991, 3947-3950.

[36] G. Rozza, D.B.P. Huynh and A.T. Patera. *Reduced Basis Approximation and a Posteriori Error Estimation for Affinely Parametrized Elliptic Coercive Partial Differential Equations.* Arch. Comput. Methods. Eng., **15**, 2008, 229-275.

[37] E.W. Sachs and S. Volkwein. *POD Galerkin approximations in PDE-constrained optimization,* GAMM Mitteilungen, **33**, 2010, 194-208.

[38] A. Sichau. *Robust Nonlinear Programming with Discretized PDE Constraints using Second-order Approximations.* PhD Thesis, TU Darmstadt, 2013.

[39] F. Tröltzsch. *Optimal Control of Partial Differential Equations: Theory, Methods and Application,* American Mathematical Society, 2010.

[40] H. Tiesler, R.M. Kirby, D. Xiu, and T. Preusser. *Stochastic Collocation for Optimal Control Problems with Stochastic PDE Constraints.* J. Control Optim., **50**, 2012, 2659-2682.

[41] F. Tröltzsch and S. Volkwein. *POD a-posteriori error estimates for linear-quadratic optimal control problems.* Computational Optimization and Applications, **44**, 2009, 83-115.

[42] S. Volkwein. *Model Reduction using Proper Orthogonal Decomposition*, Lecture Notes, University of Konstanz, 2013.

[43] M. Zahr and C. Farhat. *Progressive Construction of a Parametric Reduced-Order Model for PDE-Constrained Optimization.* Internat. J. Numer. Methods Engrg. **102**, 2015, 1111-1135.

[44] Y. Zhang. *General robust-optimization formulation for nonlinear programming.* Journal of Optimization Theory and Application, **132**, 2007, 111-124.